Computer-Aided Measurement of Breakup Processes and Tensile Strengths of Powder Beds

Computer-Aided Measurement of Breakup Processes and Tensile Strengths of Powder Beds

Keijiro TERASHITA**, Teruo KIMURA*, Hideto KIMURA* and Kei MIYANAMI**

(Received November 15, 1988)

A series of tensile tests was carried out on various kinds of powders having different moisture contents and void fractions using a hanging-cell type cohesiveness tester.

The tester is connected to a micro-computer system through an analog-to-digital conversion interface. This measurement system has allowed precise evaluation of the breakup point and breakup energy of a powder bed from its digitized breakup process curve (the relationship between tensile strength and horizontal tensile displacement). The tested powders were classified into four types by the characteristics of their breakup process curves.

1. Introduction

In processing of powders, due to adhesion, caking and bridge formation, are more encountered in fine powders and wet powders rather than in coarse powders.

Rational designing of powder processing depends on full knowledge of breakup behavior of powder beds. Therefore, detailed examinations of breakup process, tensile strength and breakup energy should be carried out on a wet powder bed using a variety of fine powders with different moisture contents. The obtained data facilitates analysis of operational processes in handling of powders.

Tensile strength of powder beds and wet powders have been formulated by Pietsch and Rumpf[6], Rumpf[7], and Schubert[8]. Cohesiveness, obtained by the equation of Rumpf[6], has been discussed by Cheng[1], Jimbo[2], and Shinohara and Tanaka[11]. Theoretical analysis of a liquid bridge has been attempted by Melrose[5], and Iinoya and Hotta[3,4]. The tensile strength of wet powders with a vast range of moisture content has been measured by Rumpf and Schubert[10]. Schubert[9] also emphasized the importance of the stress-strain relationship on breakup of powder beds and discussed the breakup process of wet powders in his studies.

In a previous analysis of the tensile breakup process curve (tensile stress – horizontal displacement) of wet powders with different moisture content, the authors have estimated the kneading condition from the tensile strength and tensile breakup energy[12,13]. However, not much has yet been achieved of systematic studies about the relationship between the breakup process and the tensile strength as well as the breakup energy in fine powders and wet powders.

Especially very little attention seems to have been paid to the studies on the breakup point of powder beds.

* Graduate Student, Department of Chemical Engineering, College of Engineering

** Department of Chemical Engineering, College of Engineering

In this paper, a computerized tensile test system was devised for more precise analysis of breakup processes of powder beds. With the aid of this system, a series of tensile tests were carried out for examination of breakup process curves under different void fractions using a large variety of fine powders and wet powders with different moisture contents.

On the basis of the obtained results, the breakup point and breakup processes were characterized by the type of powders, moisture content and void fraction. The powders were categorized by the characteristics of their breakup process curves. The breakup curves were discussed in relation to the breakup energy and tensile strength.

2. Micro-computer System

Figure 1 shows a block-diagram of the micro-computer system used in the tensile test of powder beds. Figure 2 illustrates the outline of a hanging cell type cohesiveness tester used for testing of the tensile stress. For scrupulous consideration, it is important to set the sampling interval I_s, at which to measure the tensile strength $\bar{\sigma}_x$ and horizontal displacement δ_x. In the tensile test of dry powder beds, the time course of the breakup process cannot be determined if $I_s < 0.25$ sec. On the other hand, the breakup point cannot be identified if $I_s > 0.25$ sec.

After examining the relation between I_s and breakup behavior in various combinations, I_s was set at 0.25 sec (number of integrations = 32) at which the time course of the breakup process is well delineated and the breakup point is distinctly determined.

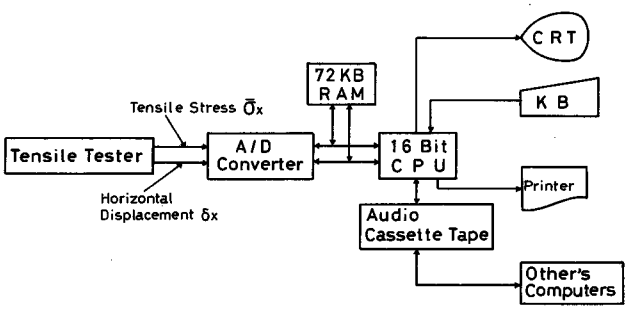

Fig. 1 Micro-computer system

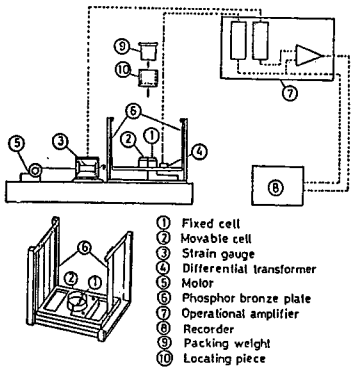

Fig. 2 Apparatus of tensile test

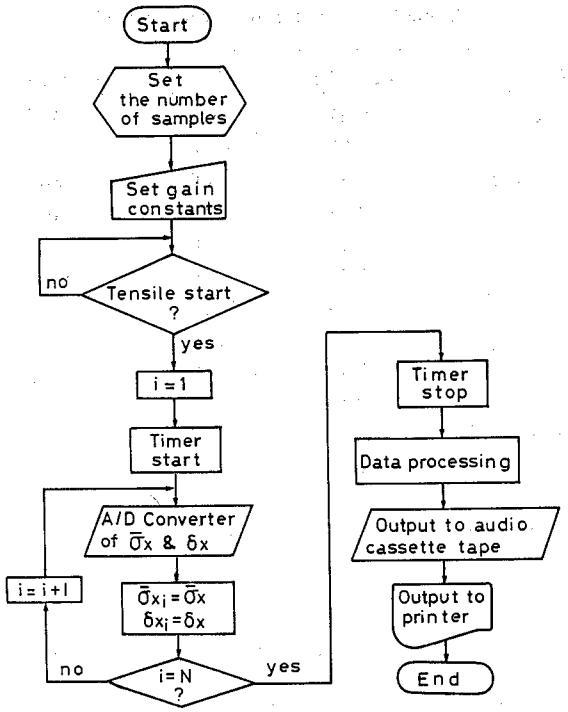

Fig. 3 Measurement flow-chart of tensile breakup process curve

In the tensile test of wet powder bed, I_s was set at 0.1 sec (number fo integrations = 28).

Figure 3 shows a flow-chart of measurement of the breakup process curves (tensile stress $\bar{\sigma}_x$ – horizontal displacement δ_x).

Simultaneously with the commencement of the measurement process, the analog-to-digital converter reads the output voltage in response to the input of the tensile stress and horizontal displacement. On termination of the measurement, the tensile stress, horizontal displacement and tensile breakup energy are computed. The computed data and breakup process curves are printed on a recording paper, and simultaneously preserved in a cassette tape. The program is for the most part constructed in BASIC. For sampling of the tensile stress $\bar{\sigma}_x$ and horizontal displacement δ_x, only A/D conversion was programmed by ASSEMBLER for the sake of rapidity and precision.

3. Experimental Method and Powder Samples

In the tensile test, a fine powder sample with a desired moisture content was packed evenly and gently in a split cell (ID 50 mm, depth 20 mm) using a spatula. After the powder bed was smoothened flat on the surface, a consolidation pressure was loaded on the bed. The pressure was released after 600 sec and the powder bed was stretched broken in a horizontal direction at a tensile velocity of 3.33×10^{-5} m/sec. The initial void fraction within the cell was adjusted by varying the vertical load consolidation pressure within the range from 1.6 to 16.1 kPa. The moisture content W_v in the wet powder was evenly distributed by complete mixing of powder and water using a vertical cylindrical mixer[12].

Table 1 Properties of powders tested

Powder	D_p [μm]	ρ [kg/m^3]	ρ_a [kg/m^3]	ϕ_r [rad]
Titanium Dioxide	0.32	3930	350	0.895
Zinc Oxide	0.73	2070	530	0.846
Kanto Loam (JIS#11)	0.82	3000	460	0.792
Corn Starch	0.97	1510	340	1.06
Sugar Powder	1.15	1510	410	0.948
Kaolin	1.25	2850	390	0.992
Lactose	1.30	1530	520	1.02
Carbon Black	1.44	1800	170	0.746
Talc	1.50	2830	590	0.878
Magnesium Stearte	1.75	1040	200	0.765
Calcium Carbonate (P-30)	1.75	2700	530	0.893
Soft Flour	1.85	1460	320	0.838
α-Alumina	1.52	3980	780	0.873
Calcium Carbonate (P-70)	22.7	2700	530	0.865

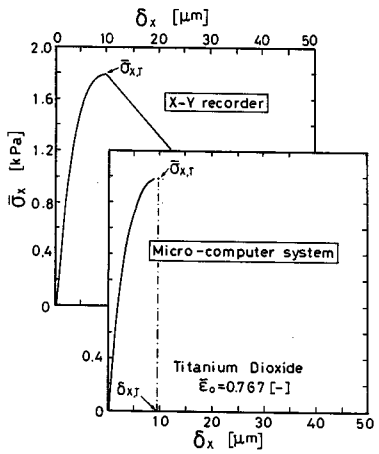

Fig. 4 Comparison of tensile breakup process curves by micro-computer system and X-Y recorder

From our previous experiments, scattering of the tensile strength was found to result from the uneveness of packing of powder cell.

Table 1 shows the fine powder samples used and their properties. In the test of wet powder, silica sand (D_p = 333 μm, ρ = 2640 kg/m^3) was used.

4. Breakup Process and Tensile Strength of Powder bed

4.1. Comparision of breakup process curves by the micro-computer system and X-Y recorder

Figure 4 shows an example of the breakup process curves obtained by the micro-computer system and X-Y recorder. The measurement by the conventional method with an X-Y recorder revealed a rapid, linear dwindling of the tensile stress $\bar{\sigma}_x$ after the peak

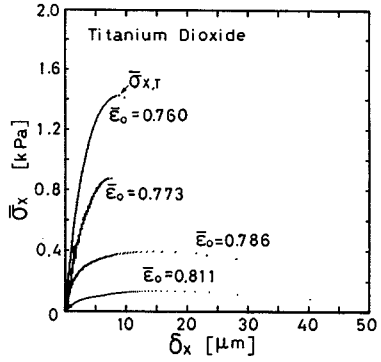

Fig. 5 Tensile breakup process curve (titanium dioxide)

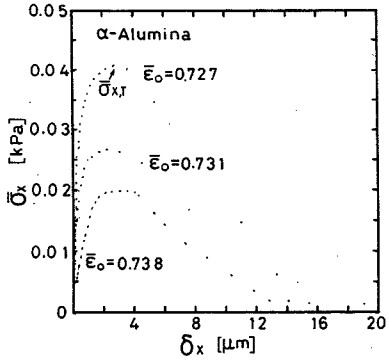

Fig. 6 Tensile breakup process curve (α-alumina)

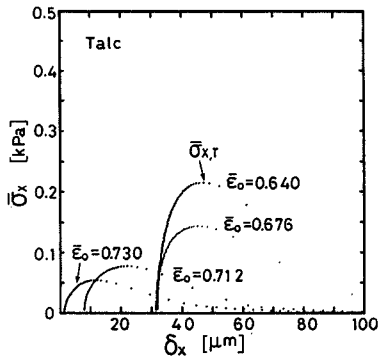

Fig. 7 Tensile breakup process curve (talc)

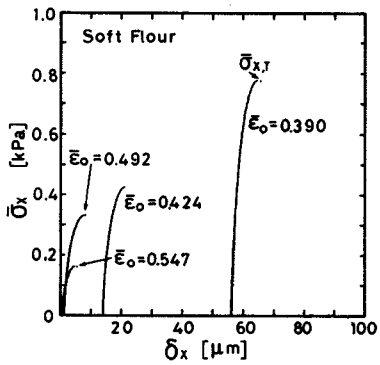

Fig. 8 Tensile breakup process curve (soft flour)

formation (= tensile strength $\bar{\sigma}_{x,T}$) due to slow response of the recorder, so it made the breakup point indeterminable. In contrast, the breakup process curve obtained by the micro-computer system clearly indicates the zero of the tensile stress $\bar{\sigma}_x$ after the peak formation ($\bar{\sigma}_{x,T}$), and demonstrates the complete breakup of the powder bed at $\bar{\sigma}_{x,T}$. The tensile strength $\bar{\sigma}_{x,T}$ is thus easily obtained.

4.2. Breakup process curves of various kinds of powder samples and categorization of fine powders

Figure 5 to 8 show examples of the breakup process curves of various powder samples with varying void fraction. A curve, with a great number of dots, appearing like a solid line indicates that breakup of the powder bed needed a long time.

In the case of titanium dioxide shown in Fig. 5, the powder bed, when compactly packed ($\bar{\varepsilon}_0$ = 0.773), is completely broken at the maximum tensile stress $\bar{\sigma}_{x,T}$ (= tensile strength) after an extremely steep intensification of the tensile stress $\bar{\sigma}_x$. When loosely packed ($\bar{\varepsilon}_0 > 0.786$), however, the dots are more widely spaced with an increase of the horizontal displacement δ_x. Such a pattern well describes the uncomplete breakup course of the powder bed, because there exist dots after indicating $\bar{\sigma}_{x,T}$. Therefore, breakup of the powder bed is obviously confirmed when compactly packed, while it is

indistinct when loosely packed.

In the case of α-alumina shown in Fig. 6, the curves are drawn with sparse dots in the early phase of breakup, indicating that breakup takes a short time. At any void fraction, the dots are present after the peak of the tensile stress. This indicates that no instantaneous breakup of the powder bed occurs even in compact packing (low void fraction).

In the case of talc shown in Fig. 7, after release of the consolidation pressure from the powder bed, the $\bar{\sigma}_x - \delta_x$ relation does not start from the original point due to spontaneous swelling (a kind of elastic property) of the powder bed. Breakup also does not occur instantaneously at any void fraction.

Soft flour has a kind of elastic property like that of talc as shown in Fig. 8. However, the breakup pattern is more simple and clear. The less the void fraction is reduced (compact packing), the higher the tensile strength $\bar{\sigma}_{x,T}$ becomes.

As shown in Fig. 9, the above results suggest two breakup mechanism; breakup of titanium dioxide (Fig. 5) when compactly packed, occurs in groups of aggregate particles (aggregate particle breakup) but when loosely packed, it is caused by disunion of individual particles (primary particle breakup). Breakup of α-alumina and talc is the pattern of primary particle breakup, because of less effect of void fraction, while aggregate particle breakup occurs in soft flour.

Figure 10 shows an example of the breakup process curves of various powder

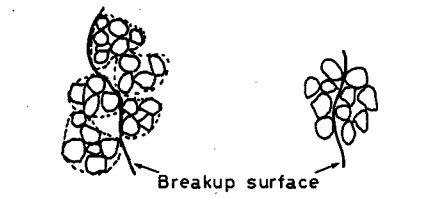

Fig. 9 Breakup patterns

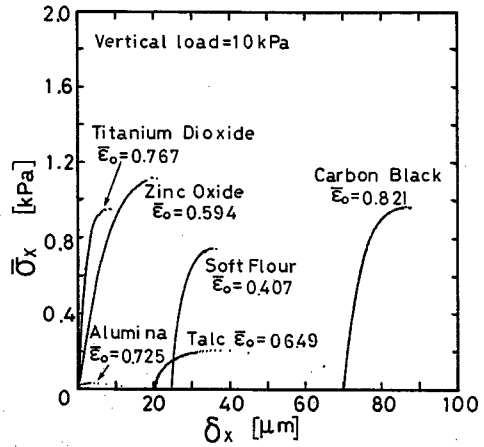

Fig. 10 Tensile breakup process curves of various powders

samples under the fixed conditions. The vertical load (consolidation pressure) was fixed at a constant value of 10 kPa. All the powder samples were compactly packed. On the basis of analysis of the breakup process curves using the A/D converter and microcomputer, fine powders were categorized into the following types.

Type I: Powders that break up like a brittle material, with an easily identifiable breakup point, showing a pattern of aggregate particle breakup (titanium dioxide, zinc oxide, calcium carbonate (P-30, P-70), magnesium stearate, corn starch, Kanto loam (JIS#1), sugar powder and lactose).

Type II: Powders that break up in a pattern similar to type I after elastic behavior in compression, showing a pattern of aggregate particle breakup (soft flour, kaolin and carbon black).

Type III: Powders that show an indeterminate breakup point and a primary particle breakup pattern (α-alumina).

Type IV: Powders that break up in a pattern similar to type III after elastic behavior in compression like type II (talc).

5. Breakup Process, Tensile Strength and Breakup Energy of Wet Powder

5.1. Breakup process curve of wet powder

Figures 11 and 12 show examples of the breakup process curve of the wet powder with varied moisture content W_V. The breakup point of silica sand in compact packing ($\bar{\varepsilon}_0 = 0.44$) shown in Fig. 11 is clearly determinable when the moisture content = 1.54% but becomes increasingly indeterminate with an increase in the moisture content. The breakup point is no longer recorded when W_V = 24.8%. On the other hand, in loose packing (Fig. 12), there exists dots at any moisture content after indicating the maximum tensile stress $\bar{\sigma}_{x,T}$. Furthermore, the horizontal displacement δ_x in response to the maximum tensile stress $\bar{\sigma}_{x,T}$ (= tensile strength) increases with an increase in the moisture content W_V regardless of the void fraction.

These results may suggest that although the liquid bridge may be elongated in compact packing as reported by Schubert *et al.*[10], the group formation of aggregate particles rather causes an indeterminate breakup point. The increase in the breakup displacement $\delta_{x,T}$ (horizontal displacement at $\bar{\sigma}_{x,T}$) with an increase in the moisture con-

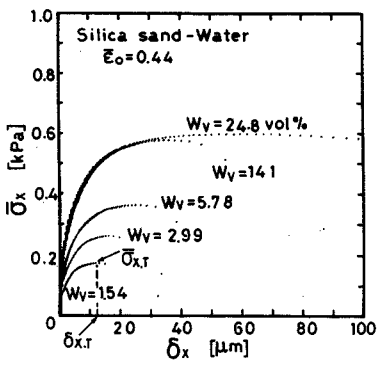

Fig. 11 Tensile breakup process curve of wet powder (void fraction $\bar{\varepsilon}_0$: 0.44)

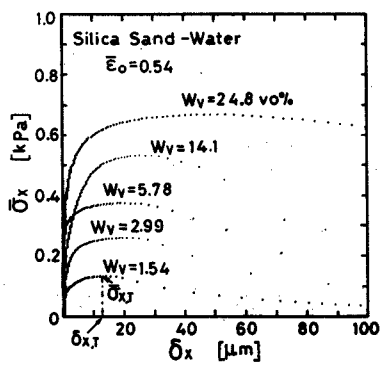

Fig. 12 Tensile breakup process curve of wet powder (void fraction $\bar{\varepsilon}_0$: 0.54)

tent may be attributed to thickening of the liquid bridge.

5.2. Tensile strength and breakup energy of wet powder

Figure 13 shows the tensile strength $\bar{\sigma}_{x,T}$ of the wet powder with different moisture content W_V. The tensile strength $\bar{\sigma}_{x,T}$ undergoes a gradual decrease with an increase in the void fraction $\bar{\varepsilon}_0$ and forms a downward bent at $\bar{\varepsilon}_0 = 0.5$, then following a rapid decrease again. Therefore, $\bar{\varepsilon}_0 = 0.5$ may correspond to the boundary between compact packing and loose packing. The increase of the moisture content may be due to swelling of the liquid bridge.

The breakup energy E_B exerted for complete breakup of the wet powder was obtained by eq. (1). The breakup energy E_T exerted for the tensile stress to reach $\bar{\sigma}_{x,T}$ was obtained by eq. (2).

$$E_B = \int_0^{\delta_{x,B}} \bar{\sigma}_x \, d\delta_x \tag{1}$$

$$E_T = \int_0^{\delta_{x,T}} \bar{\sigma}_x \, d\delta_x \tag{2}$$

Where $\delta_{x,B}$ is the horizontal displacement until complete breakup of the wet powder and $\delta_{x,T}$ the horizontal displacement at $\bar{\sigma}_{x,T}$.

Figure 14 shows E_B and E_T of the wet powder. The tensile breakup energy E_B firstly decreases with an increase in the void fraction but then gains a rapid increase at $\bar{\varepsilon}_0$ = approximately 0.5, after that, following a redecrease with a further increase in the void fraction. $\bar{\varepsilon}_0$ = approximately 0.5 may, therefore, correspond to the boundary zone between primary particle breakup and aggregate particle breakup. E_B at $W_V = 24.8\%$ showed an almost linear decrease with an increase of the void fraction. This may be probably because a large moisture content may induce aggregate particle breakup at any void fraction. The breakup energy E_B of the dry powder samples demonstrated a similar

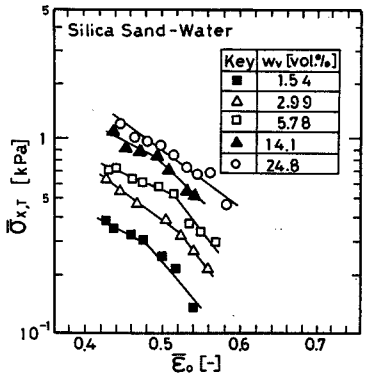

Fig. 13 Tensile strength of wet powder

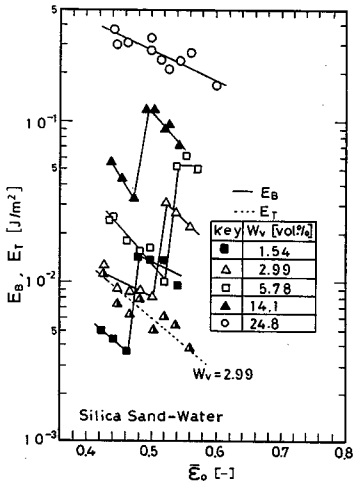

Fig. 14 Tensile breakup energy of wet powder with different moisture content

pattern of changes to that of the wet powder seen at $W_V < 14.1\%$ for titanium dioxide and zinc oxide. E_B of other dry powders showed a similar pattern to that of the wet powder seen at $W_V = 24.8\%$. Calculation of the breakup energy E_B is useful for determining the boundary between compact packing and loose packing.

6. Conclusion

A microcomputer system was introduced in tensile test of fine powders and wet powders to determine their breakup process curves, breakup energies and tensile strengths. The microcomputer system distinctly identified especially the breakup points of all the powder samples and depicted the occurence of primary particle breakup and aggregate particle breakup depending on the level of void fraction. The factors associated with these two different breakup mechanisms were distinctly discriminated by the relation between the void fraction and the breakup energy exerted for complete breakup. The boundary zone was more determinable in the wet powder than the dry powders. Fine powders were categorized by the characteristics of their breakup process curves into four types.

The relationship between the powder type and tensile strength was quantitatively analized.

Nomenclature

D_p: mass median diameter, μm
E_B: tensile breakup energy needed for complete breakup of powder bed, J/m^2
E_T: tensile breakup energy needed to obtain tensile strength, J/m^2
I_s: sampling interval, sec
S_S: standarddeviation of normal stress distribution, –
S_T: standard deviation of tensile strength, –
W_V: moisture content, vol. %
δ_x: horizontal displacement, μm
$\delta_{x,T}$: tensile breakup displacement until $\bar{\sigma}_{x,T}$, μm
$\delta_{x,B}$: displacement at complete breakup of powder bed, μm
$\bar{\epsilon}_0$: void fraction, –
ρ: particle density, kg/m^3
ρ_a: apparent density, kg/m^3
$\bar{\sigma}_x$: tensile stress, kPa
$\bar{\sigma}_{x,T}$: tensile strength, kPa
ϕ_r: angle of repose, rad

References

1) D.C.H. Cheng, Chem. Eng. Sci., **23**, 1405 (1968)
2) G. Jimbo, S. Asakawa and N. Soga, J. Soc. Materials Sci., Japan, **17**, 540 (1968)
3) K. Hotta, K. Takeda and K. Iinoya, Powder Tech., **10**, 231 (1974)
4) K. Iinoya, S. Asakawa, K. Hotta and J.H. Burson, Powder Tech., **1**, 28 (1967)
5) J.S. Melrose, AIChE J., **12**, 986 (1966)
6) W. Pietsch, and H. Rumpf, Chem-Eng-Tech., **39**, 885 (1967)
7) H. Rumpf, Chem-Eng-Tech., **42**, 538 (1970)
8) H. Schubert, Chem-Eng-Tech., **45**, 396 (1973)
9) H. Schubert, Powder Tech., **11**, 107 (1975)
10) H. Schubert, W. Herrmann and H. Rumpf, Powder Tech., **11**, 121 (1975)

11) K. Shinohara and T. Tanaka, J. Chem. Eng., Japan, 8, 50 (1975)
12) K. Terashita, K. Miyanami, T. Konishi and J. Yoshida, J. Soc. Materials Sci., Japan, **30**, 873 (1981)
13) K. Terashita, T. Kimura, H. Tsukaguchi and K. Miyanami, KONA, No. 2, 71 (1984)